crystals

MDPI

Article

High Temperature Transport Properties of Yb and In Double-Filled p-Type Skutterudites

Dean Hobbis [1], Yamei Liu [2], Kaya Wei [1], Terry M. Tritt [2] and George S. Nolas [1,*]

[1] Department of Physics, University of South Florida, Tampa, FL 33620, USA; dhobbis@mail.usf.edu (D.H.); kayawei@mail.usf.edu (K.W.)

[2] Department of Physics and Astronomy, Kinard Laboratory, Clemson University, Clemson, SC 29634, USA; yameil@g.clemson.edu (Y.L.); ttritt@clemson.edu (T.M.T.)

* Correspondence: gnolas@usf.edu; Tel.: +1-813-974-2233

Academic Editor: Helmut Cölfen

Received: 18 July 2017; Accepted: 18 August 2017; Published: 23 August 2017

Abstract: Yb and In double-filled and Fe substituted polycrystalline p-type skutterudite antimonides were synthesized by direct reaction of high-purity elements, followed by solid-state annealing and densification by hot pressing. The stoichiometry and filling fraction were determined by both Rietveld refinement of the X-ray diffraction data and energy dispersive spectroscopic analyses. The transport properties were measured between 300 K and 830 K, and basically indicate that the resistivity and Seebeck coefficient both increase with increasing temperature. In both specimens, the thermal conductivity decreased with increasing temperature up to approximately 700 K, where the onset of bipolar conduction was observed. A maximum ZT value of 0.6 at 760 K was obtained for the $Yb_{0.39}In_{0.018}Co_{2.4}Fe_{1.6}Sb_{12}$ specimen.

Keywords: thermoelectric; skutterudite; p-type; figure of merit; double-filled; bipolar diffusion

1. Introduction

Thermoelectric materials research is of current significant interest for improving device performance in order to efficiently convert waste heat into electrical power [1]. Thermoelectric device improvement would result in an expanded array of potential applications, including automobile applications [2]. The efficiency of a thermoelectric material is given by the dimensionless figure of merit $ZT = S^2T/\rho\ \kappa$, where S is the Seebeck coefficient, T is the absolute temperature, ρ is the resistivity, and κ is the thermal conductivity. The larger both the average and the peak ZT value are, the better the thermoelectric properties of a material. Both n-type and p-type materials are required in a thermoelectric device; the efficiency of the device is characterized by the combination of both materials' thermoelectric properties.

Skutterudites have been studied extensively—not only due to their encouraging thermoelectric performance at intermediate temperatures, but also due to their good mechanical properties [3–6]. Optimization of p-type skutterudites is difficult due to the relatively small effective mass of holes compared to the effective mass of electrons in these materials [4]; therefore, the optimum carrier concentration of n-type skutterudites is larger than that of p-type, leading to a larger power factor ($S^2\sigma$, where σ is electrical conductivity) [7]. It is well documented that the twelve Sb atoms in the skutterudite crystal structure form relatively large icosahedral cages [1,3,8]; thus, reduction of the lattice thermal conductivity, κ_L, can be achieved by fractional filling of these cages with rare-earth, alkali-earth, or alkali-metal atoms, since these cage-fillers result in the scattering of lattice phonons [3,8]. Yb filling has been shown to be a good filler candidate for skutterudites because of its large mass and small ionic radius, which results in strong phonon scattering. Furthermore, in skutterudites Yb has been shown to have an intermediate valence state (+2~+3), demanding less charge compensation

for p-type materials [9]. The thermoelectric properties of n-type (Yb, In) double-filled skutterudite antimonides have been previously reported with a maximum *ZT* of 0.97 [10]. The pursuit of p-type materials is also needed; herein we investigate similar double filling in p-type skutterudites in order to determine their potential for thermoelectric applications.

2. Experimental

The high-purity elements were weighed and loaded into silica crucibles in a N_2 environment inside a glove box to minimize exposure to air. Yb chunks (99.9%, Ames Labs), In foil (99.9975%, Alfa Aesar), Co powder (99.998%, Alfa Aesar), Fe powder (99.998%, Alfa Aesar), and crushed Sb chunks (99.5%, Alfa Aesar) were reacted in the nominal compositions $Yb_{0.4}In_{0.02}Co_3FeSb_{12}$ and $Yb_{0.8}In_{0.02}Co_{2.5}Fe_{1.5}Sb_{12}$ for this study, which were chosen based off of previous studies of Yb single-filled Fe substituted skutterudites [11,12]. The specimens were sealed in a quartz tube under vacuum and reacted in a furnace at 1173 K for 48 h. The tube was removed and allowed to cool to room temperature in air before the specimens were ground into fine powders in a N_2 glove box and cold pressed into pellets. These pellets were again sealed under vacuum in a quartz tube and annealed at 973 K for 7 days. This grinding and annealing process was repeated once more to further encourage homogeneity. The specimens were then finely ground and sieved (325 mesh) before being loaded into a graphite die inside the glove box for hot pressing. The hot pressing conditions for densification were performed under constant N_2 flow at 923 K and 120 MPa for 3 h, resulting in high-density polycrystalline skutterudites as measured by the Archimedes method.

Analyses of the homogeneity and stoichiometry of the specimens were performed by Rietveld refinement of the powder X-ray diffraction (XRD) data using a Bruker D8 Focus Diffractometer in Bragg–Brentano geometry with Cu Kα radiation and a graphite monochromator, and energy dispersive spectroscopy (EDS) using an Oxford INCA X-Sight 7852 equipped scanning electron microscope (SEM, JEOL, JSM-6390LV). The densified pellets were cut with a wire saw for high-temperature transport measurements. A rectangular parallelepiped ($2 \times 2 \times 5$ mm^3) was used for four-probe ρ and *S* measurements on a ULVAC ZEM-2 system. Thermal diffusivity measurements on a thin disk were performed by the laser flash method on a NETZSCH LFA 457 system, under constant Ar flow. The experimental uncertainties in both these measurements were 5–10%. Heat capacity measurements were performed using a NETZSCH DSC 404C system. Separate pieces of the specimens were also used for room-temperature Hall measurements and air stability tests. Air stability tests indicated that the specimens began to oxidize and degrade at 673 K, similar to that of previously reported skutterudites [13,14].

CCDC contains the supplementary crystallographic data for this paper, with deposition numbers 1562579 and 1562580 for $Yb_{0.13}In_{0.02}Co_3FeSb_{12}$ and $Yb_{0.39}In_{0.02}Co_{2.4}Fe_{1.6}Sb_{12}$, respectively. These data can be obtained free of charge via http://www.ccdc.cam.ac.uk/conts/retrieving.html (or from the CCDC, 12 Union Road, Cambridge CB2 1EZ, UK; Fax: +44 1223 336033; E-mail: deposit@ccdc.cam.ac.uk).

3. Results

3.1. Structural Characterization

Rietveld refinement profiles from the powder XRD data are shown in Figure 1, displaying calculated and observed data and the difference between them. Table 1 indicates the refinement results. The crystal structures were refined with space group $Im\overline{3}$ (#204), and the initial atomic positions were based on data from previously reported Yb filled skutterudites [11,12]. The filler Yb atoms at the 2*a* site occupy less than the nominal composition, due in part to a trace amount of Yb_2O_3 (observed in profiles at 29.7°) and to steric effects [11,12,15,16]. The Co-to-Fe ratios are extremely close to the nominal compositions. The lattice parameters are 9.0661 Å and 9.0877 Å for $Yb_{0.13}In_{0.02}Co_3FeSb_{12}$ and $Yb_{0.39}In_{0.02}Co_{2.4}Fe_{1.6}Sb_{12}$, respectively, with an increase in lattice parameter with Yb and In filling

fractions and Co-to-Fe ratio, in agreement with previously reported data. Furthermore, the Yb filling fraction increases from 33% to 49% with increased Fe substitution, similarly reported for Gd and (Ba, Yb) filled skutterudites [10–17]. Elemental mapping from EDS data shows an even dispersion of elements for both specimens, indicating good homogeneity of the specimens, and corroborate our refinement results.

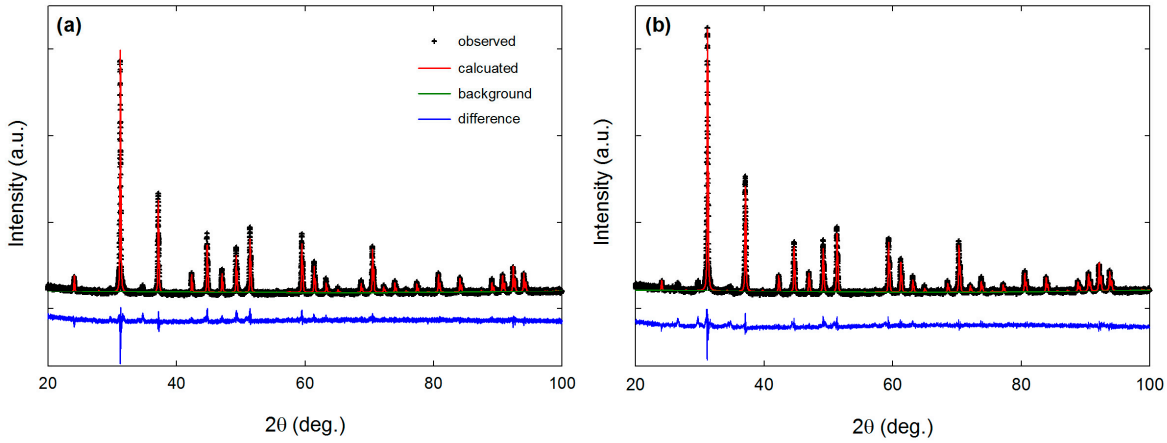

Figure 1. Powder X-ray diffraction (XRD) data for (**a**) $Yb_{0.13}In_{0.02}Co_3FeSb_{12}$ and (**b**) $Yb_{0.39}In_{0.02}Co_{2.4}Fe_{1.6}Sb_{12}$, including profile fit, profile difference, and profile residuals from Rietveld refinement.

Table 1. Rietveld refinement results for $Yb_{0.13}In_{0.02}Co_3FeSb_{12}$ and $Yb_{0.39}In_{0.02}Co_{2.4}Fe_{1.6}Sb_{12}$.

Nominal Composition	$Yb_{0.4}In_{0.02}Co_3FeSb_{12}$	$Yb_{0.8}In_{0.02}Co_{2.5}Fe_{1.5}Sb_{12}$
Composition	$Yb_{0.13}In_{0.02}Co_3FeSb_{12}$	$Yb_{0.39}In_{0.02}Co_{2.4}Fe_{1.6}Sb_{12}$
Space Group (Z)	$Im\bar{3}$ (#204), 8	
a (Å)	9.0660(6)	9.0872(8)
V (Å^3)	745.1(7)	750.4(2)
Radiation	Graphite Monochromated CuK_α (1.54056 A)	
$D_{calc.}$ (g/cm^3)	6.43	7.17
2θ range (deg.)	20–100	2–100
Step Width (deg.)	0.005	0.005
Reduced χ^2	2.40	2.84
wR_p, R_p	0.0739, 0.0581	0.0779, 0.0610
U_{iso} (Å^2) for Yb	0.0095(0)	0.0125(6)
U_{iso} (Å^2) for In	0.0090(3)	0.0101(7)
U_{iso} (Å^2) for Co/Fe	0.0070(1)	0.0039(4)
U_{iso} (Å^2) for Sb	0.0037(4)	0.0041(2)
y (Sb)	0.8436(7)	0.8423(6)
z (Sb)	0.6654(4)	0.6649(9)

Atomic Positions: Yb/In, 2a (0, 0, 0); Co/Fe, 8c (1/4, 1/4, 1/4); Sb, 24g (0, y, z).

3.2. Transport Properties

Figure 2a,b show temperature-dependent (300–800 K) S and ρ data, respectively. The $Yb_{0.13}In_{0.02}Co_3FeSb_{12}$ specimen exhibits a metallic-like temperature dependence with ρ increasing with temperature, although these values saturate to 1.6 mΩ cm^{-1} at 650 K. The ρ values for $Yb_{0.39}In_{0.02}Co_{2.4}Fe_{1.6}Sb_{12}$ do not exhibit as strong a temperature dependence in the measured temperature range. The S values for both specimens increase with increasing temperature and peak at 700 K, with values of 140 μV/K and 160 μV/K for $Yb_{0.13}In_{0.02}Co_3FeSb_{12}$ and $Yb_{0.39}In_{0.02}Co_{2.4}Fe_{1.6}Sb_{12}$, respectively. Both specimens have positive S values, indicating that holes are the majority carriers, in agreement with room-temperature Hall measurements that provide

carrier concentrations (p) of 2.6 × 10^{20} cm^{-3} and 4 × 10^{20} cm^{-3} for $Yb_{0.13}In_{0.02}Co_3FeSb_{12}$ and $Yb_{0.39}In_{0.02}Co_{2.4}Fe_{1.6}Sb_{12}$, respectively.

In the single parabolic band model, S and p are given by [18]

$$S = \pm\frac{k_B}{e}\left(\frac{(2+r)F_{1+r}(\eta)}{(1+r)F_r(\eta)} - \eta\right) \tag{1}$$

and

$$p = \frac{4\pi(2m_e k_B T)^{3/2}}{h^3}\left(\frac{m^*}{m_e}\right)^{3/2} F_{1/2}(\eta) \tag{2}$$

where the plus and minus signs in Equation (1) are for holes (+) and electrons (−), η is the reduced Fermi energy (=E_F/k_BT, where E_F is the Fermi energy, k_B is the Boltzmann constant, and T is absolute temperature), Fr is the Fermi integral of order r, and r is the exponent of the energy dependence of the electron mean free path. r = 0 for scattering from acoustic phonons (lattice vibrations) and r = 2 for ionized impurity scattering. In our estimate for effective mass, m^*, the intermediate value of r = 1 is used. Using our room-temperature S and p values, we estimate m^* to be $0.7m_e$ for $Yb_{0.13}In_{0.02}Co_3FeSb_{12}$ and $1.4m_e$ for $Yb_{0.39}In_{0.02}Co_{2.4}Fe_{1.6}Sb_{12}$. These values are much smaller than that for $Yb_xFe_{3.5}Ni_{0.5}Sb_{12}$ compositions, but are similar to $Yb_{0.5}Fe_{1.5}Co_{2.5}Sb_{12}$ and $Ca_{0.17}Ce_{0.05}Fe_{1.47}Co_{2.53}Sb_{12}$ which have a comparable Co-to-Fe content [19–21].

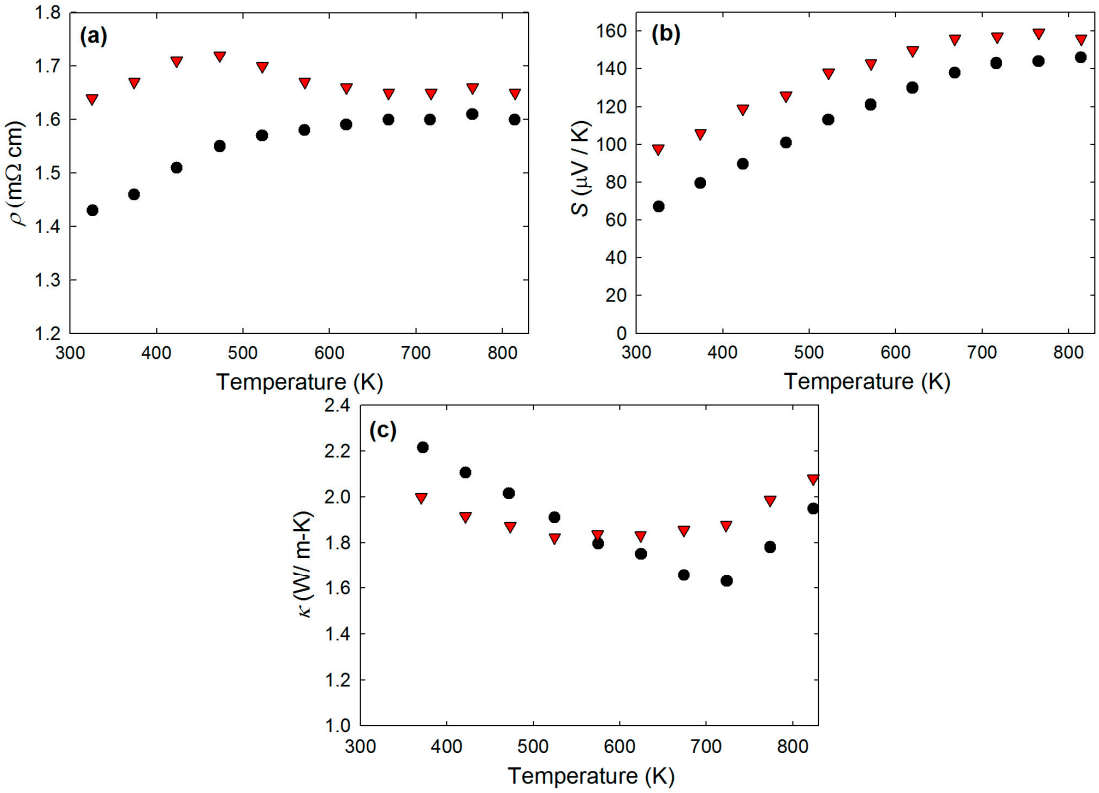

Figure 2. Temperature-dependent (**a**) ρ, (**b**) S, and (**c**) κ for $Yb_{0.13}In_{0.02}Co_3FeSb_{12}$ (circle) and $Yb_{0.39}In_{0.02}Co_{2.4}Fe_{1.6}Sb_{12}$ (triangle).

Figure 2c shows κ data calculated from thermal diffusivity and heat capacity measurements using the equation $\kappa = D{\cdot}d{\cdot}C_p$, where D is measured density, d is measured thermal diffusivity, and C_p is measured heat capacity. Figure 3 shows κ_L as calculated using the Wiedmann–Franz relation, where $\kappa_E = L_0T/\rho$ (L_0 being the Lorenz number taken to be 2.45 × 10^{-8} V^2 K^{-2}). These κ values are smaller compared to those of previously reported (Yb, In) and (Ba, In) double-filled n-type skutterudites,

as well as that of (Ce, Nd) double-filled p-type skutterudites [10,22,23]. An increase in κ and κ_L is observed above 700 K, which can be attributed to bipolar diffusion. The contribution of bipolar diffusion, κ_B, is given by $\kappa_B = \sigma_e\sigma_h(S_h\text{-}S_e)^2T/\sigma_e + \sigma_h$, where σ_e is the electron conduction, σ_h is the hole conduction, S_h is the hole Seebeck coefficient, and S_e is the electron Seebeck coefficient [1]. An estimation of κ_B can be made from the high-temperature data using $\kappa_L = 3.5(k_B/h)^3\ (MV^{1/3}\theta_D{}^3/\gamma^2T)$, where h is Planck's constant, M is the average mass per atom, V is the average atomic volume, θ_D is the Debye temperature, and γ is the Grüneisen parameter. It is clear that Umklapp scattering dominates κ_L above θ_D [1]. Therefore, the inset to Figure 3 illustrates the procedure of using a fit $\kappa_L \sim T^{-1}$ to estimate κ_B for the $Yb_{0.13}In_{0.02}Co_3FeSb_{12}$ specimen, resulting in proportions of 53%, 33%, and 14% for κ_E, κ_L, and κ_B, respectively. The estimations for the $Yb_{0.39}In_{0.02}Co_{2.4}Fe_{1.6}Sb_{12}$ specimen were done with the same method, and gave values of 48%, 44%, and 8% for κ_E, κ_L, and κ_B, respectively. These κ_B values are higher than that of single-filled Yb compositions, possibly due to the additional low-lying donor states with In filling [3,10]. An increase in Fe content resulted in a near 50% reduction in κ_B [11].

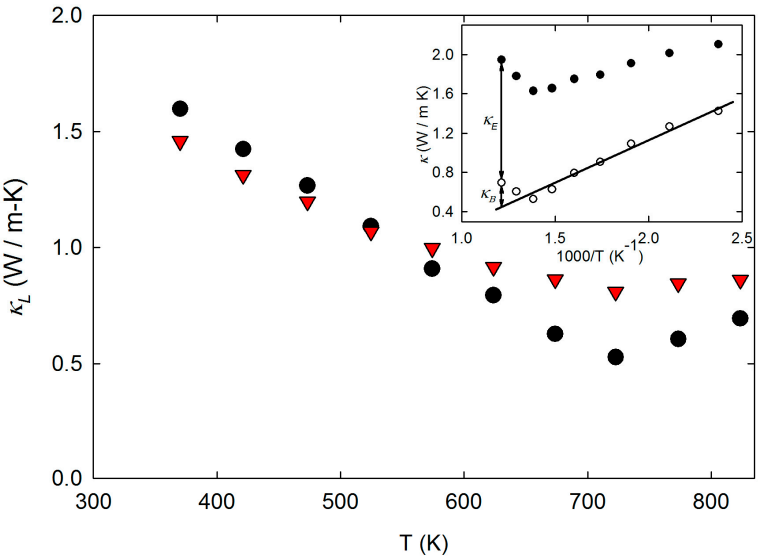

Figure 3. Temperature-dependent κ_L for $Yb_{0.13}In_{0.02}Co_3FeSb_{12}$ (circle) and $Yb_{0.39}In_{0.02}Co_{2.4}Fe_{1.6}Sb_{12}$ (triangle). The inset illustrates the method used to estimate κ_B for both specimens, with $Yb_{0.13}In_{0.02}Co_3FeSb_{12}$ shown here, where the solid line is the T^{-1} dependence between 400 K and 700 K.

Figure 4 shows the ZT values for both specimens. These values have been calculated from the measured data, and both specimens show increasing ZT with increasing temperature, with a maximum value of 0.6 at 760 K for the $Yb_{0.39}In_{0.02}Co_{2.4}Fe_{1.6}Sb_{12}$ specimen. This maximum ZT value is lower than that of the n-type (Yb, In) double-filled skutterudite but greater than (Ce, Yb) double-filled p-type skutterudites with comparable filling fraction and Co-to-Fe ratio [10,21]. However, other reported p-type (Ce, Yb) double-filled skutterudites with greater filling fraction and Fe substitution exhibit a larger ZT (=0.87) [24].

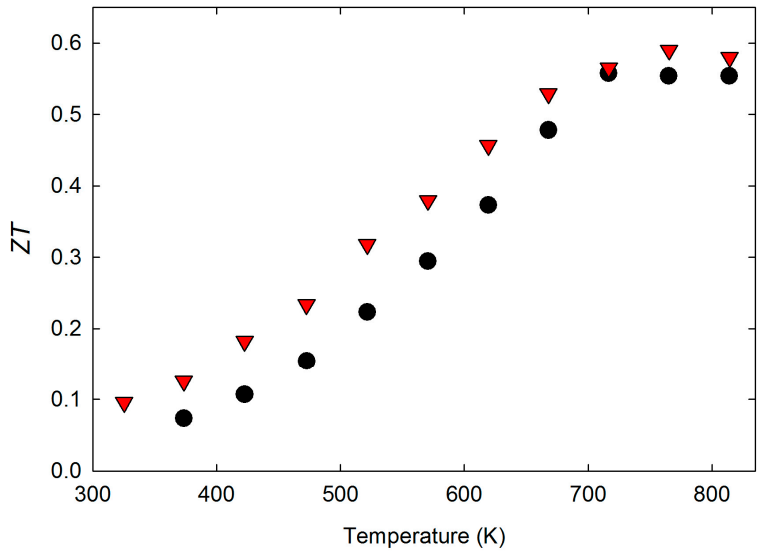

Figure 4. Temperature-dependent *ZT* for $Yb_{0.13}In_{0.02}Co_3FeSb_{12}$ (circle) and $Yb_{0.39}In_{0.02}Co_{2.4}Fe_{1.6}Sb_{12}$ (triangle).

4. Conclusions

The structural and high-temperature transport properties of p-type (Yb, In) double-filled skutterudites were investigated. We observed an increase in both ρ and S for $Yb_{0.39}In_{0.02}Co_{2.4}Fe_{1.6}Sb_{12}$, whereas κ was less for the specimen with lower Yb content. Above 700 K, both specimens exhibited a fairly large κ_B contribution that significantly increased κ above this temperature, although κ_B decreased with increasing Fe content. Both specimens exhibited the largest *ZT* values at 750 K. The performance of these p-type skutterudites may be enhanced by a further increase in overall filling fractions of (Yb, In), corresponding to an increase in Fe content.

Acknowledgments: This work was supported by the II-VI Foundation Block-Gift Program. The authors thank Jeff Sharp of Marlow Industries for air stability testing.

Author Contributions: George S. Nolas conceived and designed the experiments; Dean Hobbis and Kaya Wei performed synthesis, densification and preparation of specimens; Yamei Liu and Terry M. Tritt performed high temperature transport measurements on specimens; Dean Hobbis, Kaya Wei and George S. Nolas analyzed the data; Dean Hobbis wrote the manuscript. All authors contributed to the experiment, the analysis of the data, and edition of the manuscript.

Conflicts of Interest: The authors declare no conflict of interest.

References

1. Nolas, G.S.; Sharp, J.W.; Goldsmid, H.J. *Thermoelectrics: Basic Principles and New Material Developments*; Springer: Berlin, Germany, 2001.
2. Stabler, F.R. Commercialization of Thermoelectric Technology. *Mater. Res. Symp. Proc.* **2006**, *886*, 13–21. [CrossRef]
3. Uher, C. Skutterudites: Prospective novel thermoelectrics. In *Semiconductors and Semimetals*; Tritt, T.M., Ed.; Academic Press: San Diego, CA, USA, 2001; Volume 69, pp. 139–253; ISSN 978-0-12-752178-7.
4. Dahal, T.; Kim, H.S.; Gahlawat, S.; Dahal, K.; Jie, Q.; Liu, W.; Lan, Y.; White, K.; Ren, Z. Transport and mechanical properties of the double-filled p-type skutterudites $La_{0.68}Ce_{0.22}Fe_{4-x}Co_xSb_{12}$. *Acta Mater.* **2016**, *117*, 13–22. [CrossRef]
5. Salvador, J.R.; Yang, J.; Shi, X.; Wang, H.; Wereszczak, A.A.; Kong, H.; Uher, C. Transport and mechanical properties of Yb-filled skutterudites. *Philos. Mag.* **2009**, *89*, 1517–1534. [CrossRef]

6. Zhang, L.; Rogl, G.; Grytsiv, A.; Puchegger, S.; Koppensteiner, J.; Spieckermann, F.; Kabelka, H.; Reinecker, M.; Rogl, P.; Schranz, W.; et al. Mechanical properties of filled antimonide skutterudites. *Mater. Sci. Eng. B* **2010**, *170*, 26–31. [CrossRef]
7. Nolas, G.S.; Fowler, G. Partial filling of skutterudites: Optimization for thermoelectric applications. *J. Mater. Res.* **2005**, *20*, 3234–3237. [CrossRef]
8. Nolas, G.S.; Morelli, D.T.; Tritt, T.M. Skutterudites: A phonon-glass-electron-crystal approach to advanced thermoelectric energy conversion applications. *Annu. Rev. Mater. Res. Bull.* **1999**, *29*, 199–205. [CrossRef]
9. Nolas, G.S.; Kaeser, M.; Littleton, R.T.; Tritt, T.M. High figure of merit in partially filled ytterbium skutterudite materials. *Appl. Phys. Lett.* **2000**, *77*, 1855. [CrossRef]
10. Peng, J.Y.; Alboni, P.N.; He, J.; Zhang, B.; Su, Z.; Holgate, T.; Gothard, N.; Tritt, T.M. Thermoelectric properties of (In,Yb) double-filled $CoSb_3$ skutterudite. *J. Appl. Phys.* **2008**, *104*, 053710. [CrossRef]
11. Dong, Y.; Puneet, P.; Tritt, T.M.; Nolas, G.S. Crystal structure and high temperature transport properties of Yb-filled p-type skutterudites $Yb_xCo_{2.5}Fe_{1.5}Sb_{12}$. *J. Solid State Chem.* **2014**, *209*, 1–5. [CrossRef]
12. Dong, Y.; Puneet, P.; Tritt, T.M.; Nolas, G.S. High temperature thermoelectric properties of p-type skutterudites $Yb_xCo_3FeSb_{12}$. *Phys. Status Solidi RRL* **2013**, *7*, 418–420. [CrossRef]
13. Zhao, D.; Tian, C.; Tang, S.; Liu, Y.; Chen, L.D. High temperature oxidation behavior of cobalt triantimonide thermoelectric material. *J. Alloys Compd.* **2010**, *504*, 552–558. [CrossRef]
14. Shin, D.K.; Kim, I.H.; Park, K.H.; Lee, S.; Seo, W.S. Thermal Stability of $La_{0.9}Fe_3CoSb_{12}$. *J. Electron. Mater.* **2015**, *44*, 1858–1863. [CrossRef]
15. Dong, Y.; Puneet, P.; Tritt, T.M.; Martin, J.; Nolas, G.S. High temperature thermoelectric properties of p-type skutterudites $Ba_xYb_yCo_{4-z}Fe_zSb_{12}$. *J. Appl. Phys.* **2012**, *112*, 083718. [CrossRef]
16. Liu, R.; Chen, X.; Qiu, P.; Liu, J.; Yang, J.; Huang, X.; Chen, L. Low thermal conductivity and enhanced thermoelectric performance of Gd-filled skutterudites. *J. Appl. Phys.* **2011**, *109*, 023719. [CrossRef]
17. Zhou, C.; Morelli, D.; Zhou, X.; Wang, G.; Uher, C. Thermoelectric properties of P-type Yb-filled skutterudite YbxFeyCo4-ySb12. *Intermetallics* **2011**, *19*, 1390–1393. [CrossRef]
18. Slack, G.A.; Hussain, M.A. The maximum possible conversion efficiency of silicon-germanium thermoelectric generators. *J. Appl. Phys.* **1991**, *70*, 2694. [CrossRef]
19. Cho, J.Y.; Ye, Z.; Tessema, M.M.; Waldo, R.A.; Salvador, J.R.; Yang, J.; Cai, W.; Wang, H. Thermoelectric properties of p-type skutterudites YbxFe3.5Ni0.5Sb12 ($0.8 < x < 1$). *Acta Mater.* **2012**, *60*, 2104–2110.
20. Tang, X.; Li, H.; Zhang, Q.; Niino, M.; Goto, T. Synthesis and thermoelectric properties of double-atom-filled skutterudite compounds $Ca_mCe_nFe_xCo_{4-x}Sb_{12}$. *J. Appl. Phys.* **2006**, *100*, 123702. [CrossRef]
21. Yang, K.; Cheng, H.; Hng, H.H.; Ma, J.; Mi, J.L.; Zhao, X.B.; Zhu, T.J.; Zhang, Y.B. Synthesis and thermoelectric properties of double-filled skutterudites $Ce_yYb_{0.5-y}Fe_{1.5}Co_{2.5}Sb_{12}$. *J. Alloys Compd.* **2009**, *467*, 528–532. [CrossRef]
22. Zhao, W.; Wei, P.; Zhang, Q.; Dong, C.; Liu, L.; Tang, X. Enhanced Thermoelectric Performance in Barium and Indium Double-Filled Skutterudite Bulk Materials via Orbital Hybridization Induced by Indium Filler. *J. Amer. Chem. Soc.* **2009**, *131*, 3713–3720. [CrossRef] [PubMed]
23. Jie, Q.; Wang, H.; Liu, W.; Wang, H.; Chen, G.; Ren, Z. Fast Phase formation of double-filled p-type skutterudites by ball-milling and hot-pressing. *Phys. Chem. Chem. Phys.* **2013**, *15*, 6809–6816. [CrossRef] [PubMed]
24. Joo, G.S.; Shin, D.K.; Kim, I.H. Synthesis and Thermoelectric Properties of p-Type Double-Filled Ce1-zYbzFe4-xCoxSb12 Skutterudites. *J. Electron. Mater.* **2016**, *45*, 1251–1256. [CrossRef]